

# Breakdown of 2mm symmetry in electron diffraction from multiwalled carbon nanotubes

Zejian Liu<sup>a</sup>, Lu-Chang Qin<sup>a,b,\*</sup>

<sup>a</sup> Department of Physics and Astronomy, University of North Carolina at Chapel Hill, Campus Box 3255, Chapel Hill, NC 27599-3255, USA

<sup>b</sup> Curriculum in Applied and Materials Sciences, University of North Carolina at Chapel Hill, Chapel Hill, NC 27599-3255, USA

Received 10 November 2004; in final form 4 December 2004

Available online 24 December 2004

## Abstract

Electron diffraction patterns of single-walled carbon nanotubes always have 2mm symmetry regardless if the nanotubes themselves have such symmetry. We here show that, for the case of multiwalled carbon nanotubes, the 2mm symmetry can break down when coherent interferences of the electron waves from two different shells take place such as when two shells of the same helicity but their chiral indices ( $u,v$ ) have opposite evenness/oddity. Both an experimental electron diffraction pattern and analytic analysis are presented to demonstrate the conditions under which the 2mm symmetry breaks down in the electron diffraction patterns of multiwalled carbon nanotubes.

© 2004 Elsevier B.V. All rights reserved.

## 1. Introduction

The symmetry of electron diffraction provides deep insights in the determination and understanding of the atomic structure of materials, which governs their properties. Structure determination of carbon nanotubes, a one-dimensional nanoscale material having many extraordinary chemical and physical properties [1–3], has been a great challenge since their discovery [4]. Although electron diffraction has been playing an indispensable role in determining the atomic structure (both diameter and helicity) of carbon nanotubes [4–13], the symmetry properties of electron diffraction from carbon nanotubes have not been well studied in the literature, not to mention that there still exist controversy and confusion [14].

Single-walled carbon nanotubes are periodic in their axial direction. Due to the finite size of carbon nanotubes in the radial directions, the electron diffraction

spots are elongated perpendicular to the tubule axis and therefore form diffraction layer lines. Given the small diameter of carbon nanotubes, the kinematical theory of electron diffraction is usually sufficient to describe the scattering of electrons by carbon nanotubes [15,16]. A detailed analysis based on the kinematical theory of diffraction indicates that the electron diffraction patterns of single-walled carbon nanotubes always show 2mm symmetry even though the nanotube structure itself may not always possess such symmetry [17]. On the other hand, the inversion symmetry  $\bar{1}$  governed by the Friedel's law is always preserved in the electron diffraction patterns of carbon nanotubes.

In this Letter, we will analyze the symmetry of electron diffraction from multiwalled carbon nanotubes and give the conditions under which the 2mm symmetry is broken. An experimental electron diffraction pattern from a multiwalled carbon nanotube consisting of five concentric shells is used to demonstrate the breakdown of 2mm symmetry and the observations are explained with the aid of algebraic analysis as well as numerical simulations.

\* Corresponding author. Fax: +1 919 962 0480.

E-mail address: [lcqin@physics.unc.edu](mailto:lcqin@physics.unc.edu) (L.-C. Qin).

## 2. Theory

The atomic structure of a single-walled carbon nanotube of chiral indices  $(u,v)$ , formed by wrapping up seamlessly a graphene about a chosen axis, can be defined by the perimeter vector  $A = u\bar{a}_1 + v\bar{a}_2$  ( $\bar{a}_1$  and  $\bar{a}_2$  are the basis vectors on the graphene plane with magnitude  $a_1 = a_2 = a_0 = 0.246$  nm and inter-angle  $60^\circ$ ). A multiwalled carbon nanotube consists of multiple concentric shells with inter-tubular distances similar to the inter-planar spacing of graphite ( $\sim 0.335$  nm). The structure factor for a multiwalled carbon nanotube of  $N$  shells can be expressed as a coherent sum of the scattering amplitude from each individual shell

$$F(R, \Phi, Z) = \sum_{j=1}^N f \delta\left(Z - \frac{l_j}{c_j}\right) \sum_{n,m} \chi_j(n,m) \gamma_j(n,m) J_n(\pi d_j R) \times \exp\left[i n\left(\Phi + \frac{\pi}{2}\right)\right] \exp(i\varphi_j), \quad (1)$$

where  $(R, \Phi, Z)$  are the cylindrical coordinates in the reciprocal space,  $j$  denotes the  $j$ th tubule  $(u_j, v_j)$  of axial periodicity  $c_j$  and diameter  $d_j$ ,  $f$  is the atomic scattering amplitude of carbon for electrons,  $\varphi_j$  specifies the phase shift for the  $j$ th shell relative to the reference shell in the real space, and

$$\chi_j(n, m) = 1 + \exp\left\{2\pi i \frac{n + (2u_j + v_j)m}{3u_j}\right\}, \quad (2)$$

$$\gamma_j(n, m) = \frac{1 - \exp[-2\pi i(n + mv_j)]}{1 - \exp[-2\pi i(n + mv_j)/u_j]} = \begin{cases} u_j, & \text{if } (n + mv_j)/u_j = \text{integer} \\ 0, & \text{otherwise} \end{cases} \quad (3)$$

in which  $n$ ,  $m$  and  $l_j$  are all integers governed by the selection rule for the  $j$ th shell in the nanotube:

$$l_j = \frac{(u_j + 2v_j)n + 2(u_j^2 + v_j^2 + u_j v_j)m}{u_j M_j} \quad (4)$$

with  $M_j$  being the maximum common divisor of  $(u_j + 2v_j)$  and  $(2u_j + v_j)$ . The electron diffraction intensity distribution is  $I(R, \Phi, Z) = |F(R, \Phi, Z)|^2$ .

As a special case, for electron diffraction from single-walled carbon nanotubes, the summation over  $j$  in Eq. (1) disappears ( $N = 1$ ) and so does the subscript  $j$  in Eqs. (2)–(4).

Since the electron diffraction patterns of single-walled carbon nanotubes always possess 2mm symmetry [17], the 2mm symmetry will also be preserved in the electron diffraction pattern from a multiwalled carbon nanotube when there is no overlap of diffraction layer lines from different shells of the nanotube. This is true if none of the axial periodicities of the individual shells are commensurate with each other. On the other hand, when

the ratio of the axial periodicities of two concentric shells is a rational number, i.e., the two shells are commensurate, some diffraction layer lines will coincide and coherent interferences between the scattered electron waves from different shells will take place. The interferences between two shells produce most profound effect when the two shells have the same helicity. Under this circumstance, the two shells have the same axial periodicity and satisfy exactly the same selection rule given in Eq. (4). Since the electron diffraction intensity distribution on each layer line due to one shell is usually governed by a single Bessel function [17], the electron diffraction intensity distribution on a common layer line  $l_0$  due to both shells is

$$I(R, \Phi, l_0/c) = \chi_0^2 f^2 \{ |u_1 J_{n_1}(\pi d_1 R)|^2 + |u_2 J_{n_2}(\pi d_2 R)|^2 + 2u_1 u_2 J_{n_1}(\pi d_1 R) J_{n_2}(\pi d_2 R) \times \cos[(n_2 - n_1)(\Phi + \pi/2) + \Delta\varphi] \}, \quad (5)$$

where  $\chi_0$  is a constant determined by Eq. (2),  $n_1$  and  $n_2$  are the orders of the Bessel functions that dominate the intensity on layer line  $l_0$  from the two shells  $(u_1, v_1)$  and  $(u_2, v_2)$ , respectively,  $c$  is the common axial periodicity of the two shells, and  $\Delta\varphi = \varphi_2 - \varphi_1$  (we have assumed that these two shells have the same handedness, either both right-handed or both left-handed). From Eq. (5), we obtain that, when  $n_1$  and  $n_2$  have opposite oddity/evenness,  $I(R, \Phi + \pi, l_0) \neq I(R, \Phi, l_0)$ , i.e., the electron diffraction pattern will no longer have 2mm symmetry. Therefore, the 2mm symmetry breaks down under the condition that  $n_1 - n_2$  is an odd number except that the observation is set at certain special azimuth angles  $\Phi = (L\pi - \Delta\varphi)/(n_2 - n_1)$  ( $L$  is an integer). Otherwise,  $I(R, \Phi + \pi, l_0) = I(R, \Phi, l_0)$ , i.e., the whole electron diffraction pattern will still have 2mm symmetry.

These rules can be extended to include more than two shells of the same helicity to analyze the symmetry of the electron diffraction patterns of multiwalled carbon nanotubes for a general discussion.

## 3. Results and discussion

Fig. 1a shows a high-resolution transmission electron microscopy (HREM) image of a multiwalled carbon nanotube, which was taken with a transmission electron microscope (TEM) (JEM-2010F) operated at 80 kV to minimize possible electron irradiation damage to the nanotube. The inner and outer diameters of this nanotube are about 2.2 nm and 5.5 nm, respectively. Though the image resolution is lowered by operating the TEM at 80 kV (its optimum performance is obtained at 200 kV), it is sufficient to resolve the graphene layers to reveal that there are five walls in this carbon nanotube. An enlarged portion of Fig. 1a is shown in Fig. 1b to help

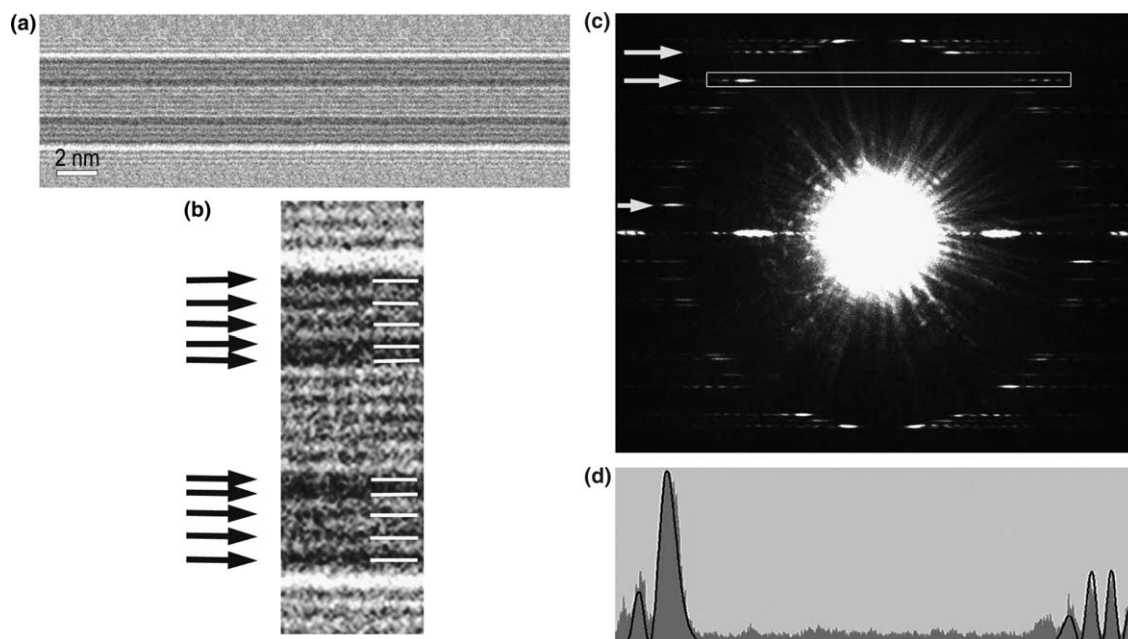


Fig. 1. (a) High-resolution transmission electron microscopy (HREM) image of a multiwalled carbon nanotube consisting of five concentric shells. The inner diameter and outer diameter of this nanotube are 2.2 and 5.5 nm, respectively. Fringes of weaker contrast are Fresnel fringes. (b) A portion the image in (a) is contrast-enhanced to show the five concentric shells. (c) Electron diffraction pattern of the carbon nanotube collected in an area of  $12 \text{ nm}^{-1} \times 10 \text{ nm}^{-1}$  in the reciprocal space. Twenty-five reflection layer lines show significant intensities and the three principal layer lines indicated by white arrows come from two shells of the same helicity. The chiral indices of all the five shells of the nanotube were determined and are given in Table 1. (d) Intensity profile of the enclosed layer line shown in (c) displaying the breakdown of 2mm symmetry. Solid line is the simulated intensity profile.

reveal in more detail that the nanotube consists of five concentric shells as indicated by the five sets of arrows around the hollow core. An electron diffraction pattern of this quintuple-walled carbon nanotube shown in Fig. 1c was obtained in the transmission electron microscope (JEM-2010F) operated at 80 kV with the incident electron beam perpendicular to the tubule axis. In the area of  $12 \text{ nm}^{-1} \times 10 \text{ nm}^{-1}$  displayed in Fig. 1c, we observed 25 layer lines of significant intensity, which can be classified into four groups by considering all the layer line spacings, each group consisting of six layer lines plus the equatorial layer line. Four helicities were identified for this quintuple-walled nanotube. A close examination of the diffraction intensities displayed in Fig. 1c reveals that the diffraction intensities on the layer lines indicated by the arrows have oscillating features. Since the three layer lines belong to one helicity, more than one nanotube must have contributed to the diffraction intensity on these layer lines, from which the helicity is determined to be  $21.6^\circ$ . We have assigned the chiral indices for each shell of this quintuple-walled carbon nanotube and the results are given in Table 1 using the method that we have developed recently. The two shells, (34,20) and (51,30), have the same helicity of  $21.5^\circ$  which falls within the range of uncertainty in our measurement.

Examination of the intensity distribution on these layer lines indicates that the mirror symmetry about

Table 1

Atomic structure of the quintuple-walled carbon nanotube shown in Fig. 1a determined from its electron diffraction pattern shown in Fig. 1c.

$(u,v)$	Metal/Semiconductor	Diameter (nm)	Helicity (DEG)
(22,9)	S	2.16	16.4
(33,6)	M	2.85	8.2
(34,20)	S	3.70	21.5
(53,12)	S	4.69	10.0
(51,30)	M	5.55	21.5

equatorial plane or the axial direction is no longer present in the layer lines marked with arrows and therefore the whole diffraction pattern does not have 2mm symmetry. The breakdown of 2mm symmetry in the electron diffraction pattern in Fig. 1c can be understood from Eq. (5) and the rules developed above. For the three principal layer lines (formed by the  $\{100\}^*$  type principal reflections of graphene) indicated by arrows in Fig. 1c, the crystallographic indices of the three layer lines from top to bottom are  $l_1 = (2u + v)/M = 44$ ,  $l_2 = (u + 2v)/M = 37$ , and  $l_3 = (u - v)/M = 7$ , respectively. For layer line  $l_1$ ,  $n_1 = 20$  and  $n_2 = 30$ , respectively, and  $n_2 - n_1 = -10$  is an even number. Therefore, the mirror symmetry is preserved about the tubule axis for this layer line. However, for layer lines  $l_2$  ( $n_1 = 34$ ,  $n_2 = 51$  and  $n_2 - n_1 = 17$ ) and  $l_3$  ( $n_1 = -54$ ,  $n_2 = -81$  and  $n_2 - n_1 = -27$ ), the mirror symmetry breaks down, as

shown in the electron diffraction pattern shown in Fig. 1c. Fig. 1d shows the intensity profile of the enclosed region (layer line  $l_2$ ) in Fig. 1c to illustrate the profound asymmetry about the tubule axis. Calculated intensity profile using Eq. (5) is plotted in solid line for comparison with the experimental data and they are in good agreement.

We have also constructed a double-walled carbon nanotube composed of two concentric shells of the same helicity with chiral indices (34,20) and (51,30), respectively, depicted as Fig. 2a, to perform numerical simulations of the electron diffraction intensity distribution. By varying the azimuth angle  $\Phi$  in observation and the relative phase shift between the two shells, we have calculated a series of electron diffraction patterns from the model structure. Fig. 2b displays a typical simulated electron diffraction pattern which matches the experimental data very well, where layer line  $l_1$  is symmetrical, while layer lines  $l_2$  and  $l_3$  are asymmetrical about the vertical axis and the equatorial plane.

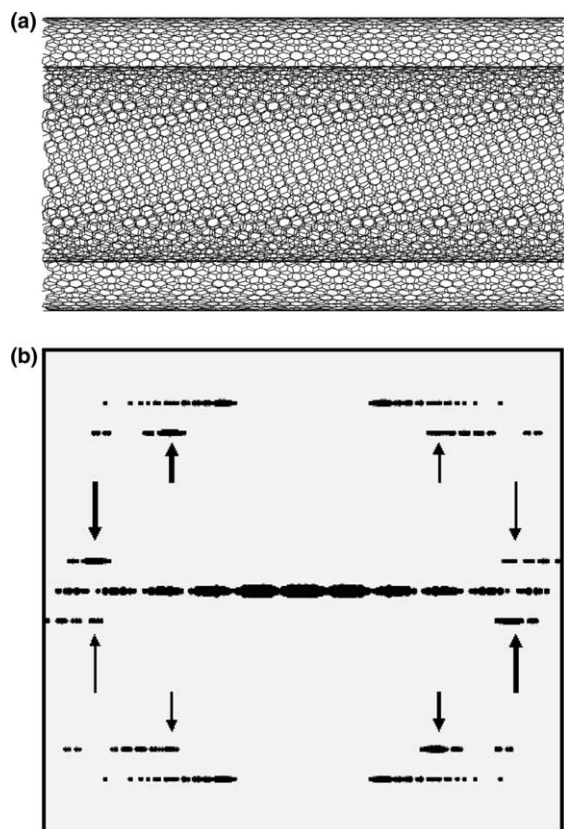


Fig. 2. Simulated two-dimensional electron diffraction pattern of a nanotube composed of two concentric shells of the same helicity with chiral indices (34,20) and (51,30), respectively. (a) Side view of the model structure of the nanotube. (b) Simulated electron diffraction pattern of the model structure shown in (a). Arrows indicate intensities that are no longer symmetrical about the equatorial plane and the vertical central axis.

When two shells have commensurate periodicities but different helicities in a multiwalled carbon nanotube, the overlapping layer lines may not be necessarily the three principal layer lines  $l_1$ ,  $l_2$ , and  $l_3$  as shown schematically in Fig. 2b. Though Eq. (5) is still valid, the experimentally observed intensities on these layer lines are usually much weaker than the principal layer lines, and therefore the loss of 2mm symmetry would not be as apparent as in the case discussed above.

#### 4. Conclusions

The 2mm symmetry of electron diffraction from multiwalled carbon nanotubes breaks down when coherent interferences of the electron waves from two different shells take place such as in the case when two shells are of the same helicity but their chiral indices ( $u,v$ ) have opposite evenness/oddity. An experimental electron diffraction pattern of a quintuple-walled carbon nanotube has been analyzed to corroborate the theoretical analysis of symmetry breaking, which is further demonstrated in the simulated electron diffraction from a double-walled carbon nanotube with both shells having the same helicity. Observation of 2mm symmetry breaking in the electron diffraction pattern can also be very helpful to resolve the atomic structure of multiwalled carbon nanotubes.

#### References

- [1] R. Saito, G. Dresselhaus, M.S. Dresselhaus, *Physical Properties of Carbon Nanotubes*, Imperial College Press, London, 1998.
- [2] P. Avouris, *Acc. Chem. Res.* 35 (2002) 1026.
- [3] M.S. Strano, C.A. Dyke, M.L. Usrey, P.W. Barone, M.J. Allen, H.W. Shan, C. Kittrell, R.H. Hauge, J.M. Tour, R.E. Smalley, *Science* 301 (2003) 1519.
- [4] S. Iijima, *Nature (London)* 354 (1991) 56.
- [5] S. Iijima, T. Ichihashi, *Nature (London)* 363 (1993) 603.
- [6] L.-C. Qin, T. Ichihashi, S. Iijima, *Ultramicroscopy* 67 (1997) 181.
- [7] L.-C. Qin, S. Iijima, H. Kataura, Y. Maniwa, S. Suzuki, Y. Achiba, *Chem. Phys. Lett.* 268 (1997) 101.
- [8] J.M. Cowley, P. Nikolaev, A. Thess, R.E. Smalley, *Chem. Phys. Lett.* 265 (1997) 379.
- [9] L.-C. Qin, *Chem. Phys. Lett.* 297 (1998) 23.
- [10] J.-F. Colomer, L. Henrard, P. Lambin, G. Van Tendeloo, *Euro. Phys. J. B* 27 (2002) 111.
- [11] M. Kociak, K. Suenaga, K. Hirahara, Y. Saito, T. Nakahira, S. Iijima, *Phys. Rev. Lett.* 89 (2002) 155501.
- [12] M. Gao, J.M. Zuo, R.D. Twisten, I. Petrov, L.A. Nagahara, R. Zhang, *Appl. Phys. Lett.* 82 (2003) 2703.
- [13] J.M. Zuo, I. Vartanyants, M. Gao, R. Zhang, L.A. Nagahara, *Science* 300 (2003) 1419.
- [14] S. Amelinckx, A.A. Lucas, P. Lambin, *Rep. Prog. Phys.* 62 (1999) 1471.
- [15] L.-C. Qin, *J. Mater. Res.* 9 (1994) 2450.
- [16] A.A. Lucas, V. Bruyninckx, P. Lambin, *Europhys. Lett.* 35 (1996) 355.
- [17] Z. Liu, L.-C. Qin, *Chem. Phys. Lett.* 400 (2004) 430.